DOI: 10.61782/fa.2023.0987

forum acusticum 2023

INVESTIGATION OF ACOUSTIC BACK-COUPLING IN HUMAN PHONATION VIA PARTICLE IMAGE VELOCIMETRY

Christoph Näger[1*] **Stefan Kniesburges**[2] **Stefan Becker**[1]

[1] Institute of Fluid Mechanics, Friedrich-Alexander-Universität Erlangen-Nürnberg, Germany

[2] Division of Phoniatrics and Pediatric Audiology at the Department of Otorhinolaryngology, Head and Neck Surgery, University Hospital Erlangen, Medical School at Friedrich-Alexander-Universität Erlangen-Nürnberg, Germany

ABSTRACT

A detailed investigation of the interaction between fluid flow and acoustics in the human voice is often hindered due to limited access to the flow field in the larynx and trachea. Especially the influence of vocal tract (VT) acoustics on the flow field and the vocal fold (VF) oscillation is not yet fully understood. Therefore, we studied acoustic back-coupling using a synthetic larynx model. High-speed particle image velocimetry measurements were performed in the supraglottal region of our model. To study the influence of VT acoustics on the supraglottal flow field in a systematic way, we employed a variable-length VT to change its acoustic resonant frequencies in relation to the VF oscillation frequency f_o. Dynamic mode decomposition was applied, which allowed us to quantify changes in the coherent structures of the flow field with changing VT acoustics. The acoustical properties of the VT were determined in advance using a transmission line model. We were not able to find acoustic feedback on the flow field for all configurations. The strongest influence of vocal tract acoustics was observed when f_o was close to a VT resonant frequency. In this case, a shift of f_o towards the resonant frequency took place.

Keywords: *human phonation, particle image velocimetry, dynamic mode decomposition*

**Corresponding author*: christoph.naeger@fau.de.

1. INTRODUCTION

The human voice is generated in a complex interplay of fluid flow, structural vibration, and acoustics. In this process, the vocal folds (VF) are stimulated to vibrate by a flow of air $\dot{V}$ from the lungs. This oscillation in turn leads to a modulation of the air flow, resulting in a pulsating jet flow in the vocal tract (VT). The sound that constitutes the voice thereby arises aeroacoustically from the turbulent free jet, as well as vibroacoustically by sound radiation from the vocal fold surface. This sound is filtered through the vocal tract and radiated through the mouth, resulting in the voice. For a long time, a linear behavior between sound source and filter was assumed, i.e., changes in the source induced by changes in the filter were neglected [1]. However, this simplified representation is not always valid, epsecially when a resonant frequency f_R of the VT is close to the oscillation frequency of the vocal folds f_o [2]. This has been studied in the past using theoretical modeling (e.g. [3]), simulations (e.g. [4–6]), in vivo studies (e.g. [7, 8]), and ex vivo and in vitro experiments (e.g. [9–11]). However, due to the complexity of the problem, often only simple metrics such as f_o-variation or the change in the oscillation threshold pressure have been studied. Particle Image Velocimetry (PIV) is a measurement technique that allows a detailed insight into the dynamics of a fluid flow. As such, it has already been proven to be a useful method to study the aerodynamics involved in human phonation. Classical planar PIV measurements allowed to study the basic features of the supra- and intraglottal aerodynamics [12–14]. The emergence of high-speed PIV made it possible to directly analyze aeroacoustic source terms computed from PIV measurements and gain insight into the location of acoustic sources in-

side the VT [15, 16]. Even tomographic PIV measurements have been applied in voice research recently, allowing to study volumetric quantities such as the maximum flow declination rate [17]. However, none of these techniques have been used yet to investigate the effect of supraglottal acoustics on the glottal aerodynamics yet. Therefore, to gain a detailed insight into the interaction between vocal tract acoustics and aerodynamics, particle image velocimetry (PIV) was applied in this work to analyze the supraglottal flow field for different vocal tract lengths. Varying the length thereby changed the acoustic properties of the vocal tract, allowing a systematic investigation of the relationship between flow and acoustics.

2. METHODOLOGY

Synthetic vocal folds were cast from a single layer of silicone. Their shape was based on the M5 model [18, 19] and is displayed in Fig. 1. The entire experimental setup is shown schematically in Fig. 2. The flow through the

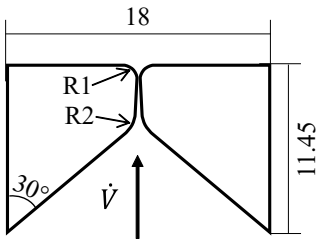

Figure 1. The vocal fold model used with its dimensions given in mm. The flow direction in the experiment is indicated.

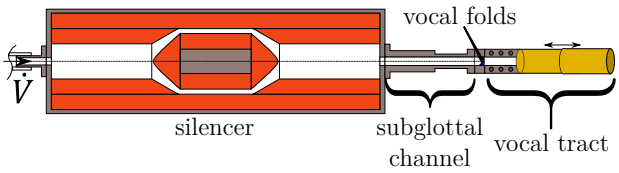

Figure 2. The experimental setup. The vocal fold position is indicated between the vocal tract and the subglottal channel. A silencer is placed upstream to attenuate emerging sound in the inflow hose.

setup was from left to right as indicated in the figure. The

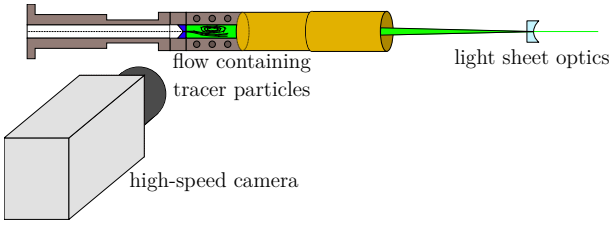

Figure 3. The setup for the PIV measurements. Visualization of the flow was performed using tracer particles and laser double pulses. The rectangular section of the vocal tract provided optical access through a glass window, allowing the flow to be recorded with a high-speed camera.

vocal folds were located between the VT and the subglottal channel. The VT consisted of two sections: the first section was a rectangular channel that had the same cross-section as the vocal folds. Connected to it was a second channel with a circular cross-section, consisting of two telescopic tubes. This made it possible to continuously vary the length of the vocal tract, allowing its acoustic resonant frequencies to be adjusted. PIV measurements were performed for different vocal tract lengths L in the range $L \in [200, 800]\mathrm{mm}$. This way, the influence of the vocal tract resonant frequencies on the supraglottal flow field was investigated. The PIV setup is shown in Fig. 3. The measurement frequency was $2 \times 5\,\mathrm{kHz}$ at a pulse distance of $\Delta t = 4\,\mu\mathrm{s}$ and a total measurement time of $1\,\mathrm{s}$ per investigated VT length.

The acoustic properties of the VT were determined in advance using a transmission line model [20]. For this purpose, the vocal tract was divided into sections of equal cross-section, allowing the frequency-dependent VT input impedance Z_{in} to be calculated via matrix chain multiplication. The maxima of Z_{in} thereby corresponded to the VT resonant frequencies. The transmission line model was implemented following the description given by Story et al. [21]. As the VT walls were fabricated from aluminium and glass, they were modeled as rigid walls. The radiation impedance at the open end was approximated as a vibrating piston in an infinite baffle [22].

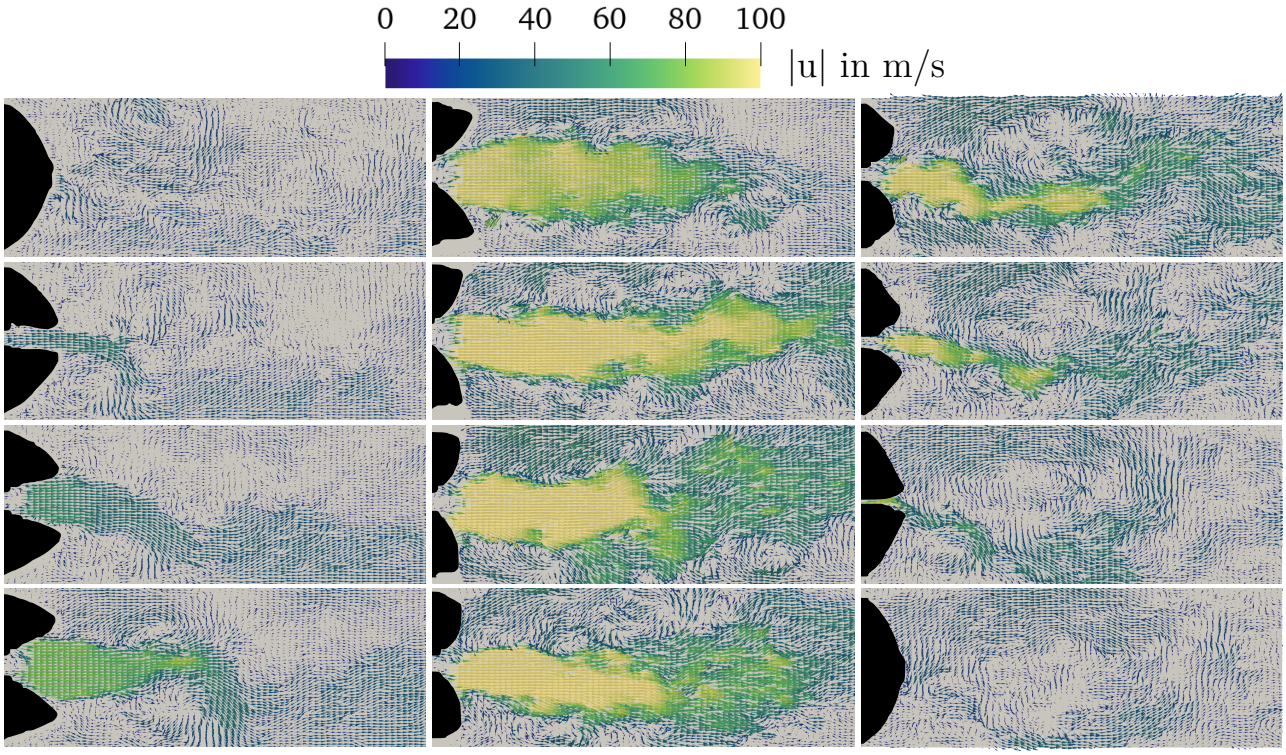

Figure 4. Instantaneous flow fields for 12 different time steps. The time steps of the snapshots are distributed equidistantly over one oscillation period, in temporal order from top to bottom and from left to right.

3. RESULTS

3.1 Analysis of the flow field

At first, the flow field at the base VT length of $L = 200\,\mathrm{mm}$ is be analyzed. Fig. 4 shows the instantaneous flow fields for $L = 200\,\mathrm{mm}$ for 12 different time steps. Here, the position of the vocal folds is overlaid in black, indicating the current phase of oscillation. The basic characteristic of the flow is an oscillating jet with an oscillation frequency of $f_o = 151\,\mathrm{Hz}$. It is evident from the figure that the jet flow is deflected toward the lower channel wall during the closing phase of the VF oscillation. This leads to the formation of a large-scale vortex in the VT during the closed phase. In other periods of the VF oscillation, this deflection also occurred toward the upper channel wall (not shown). This also resulted in a changed rotational direction of the vortex in the closed phase. It can also be seen that the oscillating jet flow is highly turbulent. As a result, the large, coherent structures underlying the flow are masked by small-scale turbulent structures.

To be able to analyze the coherent structures anyway, a dynamic mode decomposition (DMD) [23] is applied to the measured flow fields. The DMD spectrum is displayed in Fig. 5. It is apparent, that the spectrum is dominated by the oscillation frequency at $f_o = 151\,\mathrm{Hz}$ and its corresponding higher harmonics at $2f_o, 3f_o, 4f_o$ etc. Furthermore, there are two broadband peaks visible centered at approximately $f = 45\,\mathrm{Hz}$ and $f = 110\,\mathrm{Hz}$. For the analysis of these components, five reconstructed modes are shown in Fig. 6. Here, the mode of the fundamental frequency (151 Hz) describes the basic oscillatory behavior of the jet. It exhibits high velocities in the opening phase of the VFs, while showing velocities close to zero in the closed phase. In the open phase, two vortices also form above and below the jet between the two channel walls and the large velocity region in the center of the channel, which is visualized by the stream lines in the right frame. In this fundamental mode, the jet is symmetrical over the

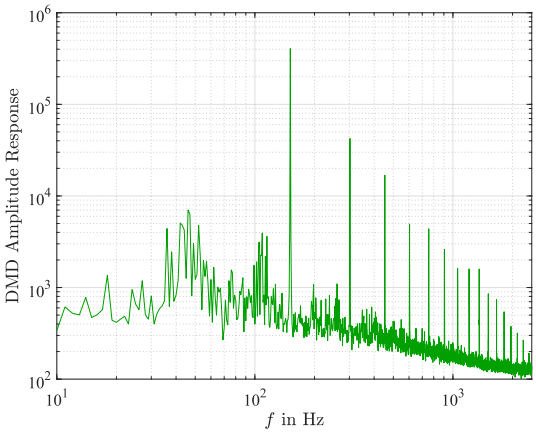

Figure 5. DMD spectrum for $L = 200\,\mathrm{mm}$. Negative frequencies are omitted due to symmetry of the spectrum.

entire period, i.e., the deflection of the jet to one of the channel walls is not described by this mode, nor is the large scale circulation in the VT during the closed phase of the VFs. Instead, these two features of the flow can be explained by the modes corresponding to the broadband peaks in the DMD spectrum at 45 Hz and 110 Hz. The top frames in Fig. 6 show the mode at 45 Hz exemplarily. While the mode at 110 Hz is not shown, it exhibits a very similar behavior to the mode at 45 Hz and differs only in its corresponding frequency. Both modes show a large-scale vortex extending over the entire measurement region, that reverses its direction of rotation at the respective frequency (indicated in the figure by the reversed arrow direction on the streamlines between the two frames). This vortex interacts with the jet in the open states and results in the deflection that can be seen in Fig. 4. At the same time, it is also responsible for the circulation of the flow in the closed phase. As described above, the deflection of the jet can occur both to the upper and to the lower channel wall. The respective direction depends on the direction of rotation of the vortex from the low frequency modes. Since the number of preiods in the real flow case, until a change of direction occurs can vary, this mode is not characterized by a single frequency but by a range of frequencies. This is the reason, why this mode shows up as a broadband distribution in the DMD spectrum of Fig. 5. The modes at 302 Hz, 453 Hz, and 604 Hz in Fig. 6 are qualitatively similar to each other. All of them show pairs of vortices, that are detached at the vocal folds. It is evident, that the spatial dimensions of the vortices decrease with increasing frequency (in the figure from top to bottom). The vortices are subsequently convected along the shear layer of the jet. The same behavior is observed for the even higher harmonics of the flow, which are not plotted within Fig. 6. These vortex pairs -superimposed with the oscillating jet- result in a high-frequency pulsation of the jet. Due to the fact, that the vortex-centers are not always perfectly aligned, these modes also result in a high-frequency "shaking" of the jet during the VF open phase.

3.2 Influence of acoustics on the flow

A DMD analysis of the flow fields at other vocal tract lengths shows that there is no qualitative change in the behavior of the modes underlying the flow. Again, the f_o mode describes the oscillation of the free jet, while the higher harmonics are characterized by detachment of vortex pairs of different sizes. The low-frequency, large scale vortex responsible for the deflection of the jet is also present in all configurations. In order to investigate the influence of acoustics on the flow field, it is necessary to determine the acoustic properties of the VT as a function of its length. For this purpose, the vocal tract input impedance Z_{in} was determined using a transmission line model. The maxima of Z_{in} are located at the acoustic resonant frequencies of the vocal tract. Fig. 7 shows Z_{in} as a function of frequency f and VT length L. Two resonant frequencies are visible in the displayed range up to 500 Hz. Both decrease in frequency with increasing length. Their frequency is slightly higher than what would be expected from classical quarter-wave resonator theory, which can be explained by the impedance jump that occurs at the position, where the channel cross section changes from rectangular to circular. Also plotted in Fig. 7 is the variation of f_o with changing L. f_o was extracted manually from the DMD spectra of the corresponding PIV measurements for this. It can be seen that there is a range $L < 400\,\mathrm{mm}$ where f_o is independent of the resonant frequencies. In this range, f_o varies minimally between 151 Hz and 153 Hz, with variations of this magnitude attributable to slight changes in the experimental conditions, such as mean volume flow rate or transglottal pressure. In the range $L \geq 600\,\mathrm{mm}$, it is clear that f_o matches the first resonant frequency of the vocal tract. Thus, as L increases, f_o decreases uniformly with

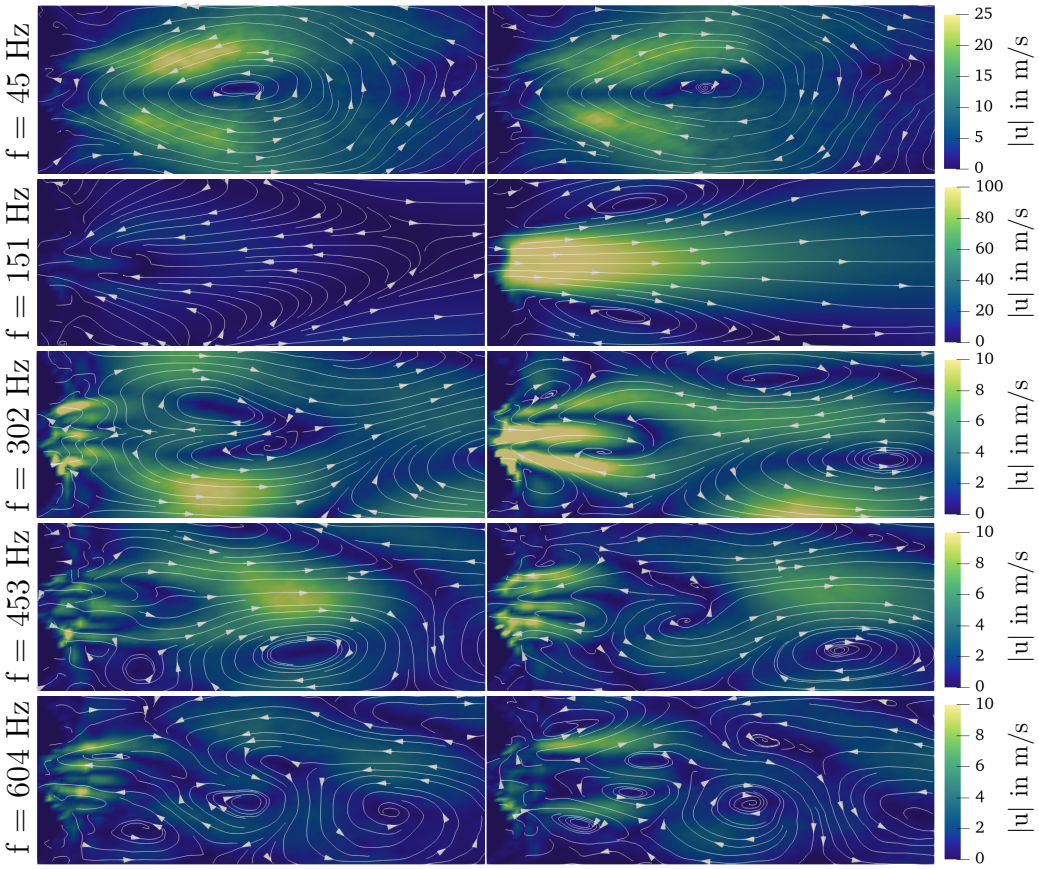

Figure 6. Reconstruction of five DMD modes. Each image pair belongs to one mode with the frequency indicated on the left border. The mode at $f = 151\,\mathrm{Hz}$ additionally includes the average flow field.

resonant frequency. This suggests that the fundamental oscillation frequency of the jet is directly affected by the standing acoustic waves present in the VT. This f_o-shift thereby also affects the higher harmonics, which are also shifted to the same extent. This means that the VT acoustics also influence the vortex pairs detected by the DMD (Fig. 6). A f_o reduction implies for the vortex pairs that either their detachment frequency and thus the distance of the vortices to each other, or their convection velocity must decrease as a result. A noteworthy anomaly occurs at $L = 400\,\mathrm{mm}$. Here f_o shifts much earlier to the acoustic resonant frequency, leading to an increase of f_o by a factor of about 1.5 to a frequency of 226 Hz. This f_o increase is not seen at $L = 500\,\mathrm{mm}$. A possible explanation for this phenomenon could be the eigenmodes of the VF model. A natural frequency at about 226 Hz may cause the vibrational mode of the VFs to change to the associated natural mode, since the acoustic resonant frequency of the VT favors it at $L = 400\,\mathrm{mm}$. Indicative of this is that this change in the vibrational mode of the VFs was already observed in a previous work using high-speed camera recordings [24] (source in German). A further indication is given by the DMD spectrum for $L = 400\,\mathrm{mm}$ (Fig. 8). Here it can be seen that in addition to the clearly highlighted peaks at f_o, $2f_o$, $3f_o$ etc there are also smaller peaks at $f_o/3$, $2f_o/3$ etc. This indicates that not only has there been a shift in f_o, but also new tonal components have been added. At $L = 500\,\mathrm{mm}$, the resonant frequency is again too far from the natural frequency of the VF model, so that here f_o is again at approx. 150 Hz, the VF model switches back to the original mode of oscillation.

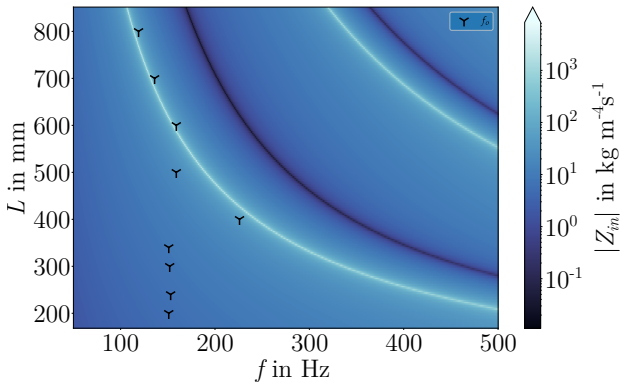

Figure 7. The vocal tract input impedance as a function of frequency f and length L. Superimposed are the oscillation frequencies f_o at the individual measurements.

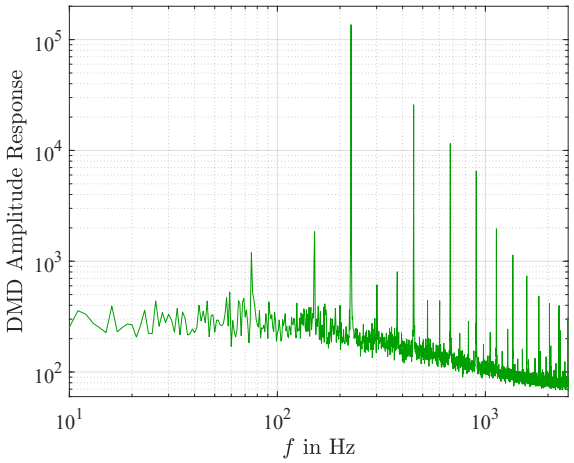

Figure 8. DMD spectrum for $L = 400\,\mathrm{mm}$. Negative frequencies are omitted due to symmetry of the spectrum.

4. SUMMARY AND CONCLUSION

The aerodynamics in the VT were shown to be characterized by a fundamental oscillation and higher-frequency pulsations due to periodically detaching vortex pairs. A large-scale vortex extending over the entire measurement area causes a deflection of the jet toward the upper or lower channel walls. Furthermore, a clear influence of the acoustic waves in the vocal tract on the flow could be detected. As the VT resonant frequency approaches f_o, f_o is "pulled" to the resonant frequency. This results in a changed fundamental frequency of the jet flow and changed vortex shedding behavior. In addition, a natural frequency-induced change in the vibration mode of the VFs could be detected when the resonant frequency of the VT is close to a natural frequency of the VFs. However, to confirm this finally, a modal analysis of the VF model used must be performed in the future. There remain other questions to be addressed in the future: first, one issue is the extent to which the observed effects in the flow affect the aeroacoustic sound generation in the VT. For this, a source term analysis from the PIV measurements with an acoustic analogy as performed by Lodermeyer et al. [15, 16] may help. Another open question is to what extent the obtained findings can be applied to the understanding of in vivo practice. In this regard, the case of the singing voice is particularly relevant, since interactions between acoustics and flow could be observed especially when f_o was close to an acoustic resonant frequency of the VT. However, this case usually does not occur in normal speaking voices, where f_o is generally much lower than the first resonant frequency.

5. ACKNOWLEDGMENTS

This work is funded by the German Research Foundation (DFG) through the project "Tracing the mechanisms that generate tonal content in voiced speech". Project number: 446965891.

6. REFERENCES

[1] G. Fant, *Acoustic Theory of Speech Production*. DE GRUYTER, 12 1971.

[2] I. R. Titze, "Nonlinear source–filter coupling in phonation: Theory," *The Journal of the Acoustical Society of America*, vol. 123, pp. 2733–2749, 5 2008.

[3] R. S. McGowan and M. S. Howe, "Source-tract interaction with prescribed vocal fold motion," *The Journal of the Acoustical Society of America*, vol. 131, pp. 2999–3016, 4 2012.

[4] M. Zañartu, L. Mongeau, and G. R. Wodicka, "Influence of acoustic loading on an effective single mass

model of the vocal folds," *The Journal of the Acoustical Society of America*, vol. 121, pp. 1119–1129, 2 2007.

[5] J. C. Lucero, K. G. Lourenço, N. Hermant, A. V. Hirtum, and X. Pelorson, "Effect of source–tract acoustical coupling on the oscillation onset of the vocal folds," *The Journal of the Acoustical Society of America*, vol. 132, pp. 403–411, 7 2012.

[6] B. D. Erath, S. D. Peterson, K. S. Weiland, M. W. Plesniak, and M. Zañartu, "An acoustic source model for asymmetric intraglottal flow with application to reduced-order models of the vocal folds," *PLOS ONE*, vol. 14, p. e0219914, 7 2019.

[7] L. Wade, N. Hanna, J. Smith, and J. Wolfe, "The role of vocal tract and subglottal resonances in producing vocal instabilities," *The Journal of the Acoustical Society of America*, vol. 141, pp. 1546–1559, 3 2017.

[8] M. Echternach, C. T. Herbst, M. Köberlein, B. Story, M. Döllinger, and D. Gellrich, "Are source-filter interactions detectable in classical singing during vowel glides?," *The Journal of the Acoustical Society of America*, vol. 149, pp. 4565–4578, 6 2021.

[9] Z. Zhang, J. Neubauer, and D. A. Berry, "Influence of vocal fold stiffness and acoustic loading on flow-induced vibration of a single-layer vocal fold model," *Journal of Sound and Vibration*, vol. 322, pp. 299–313, 4 2009.

[10] B. L. Smith, S. P. Nemcek, K. A. Swinarski, and J. J. Jiang, "Nonlinear source-filter coupling due to the addition of a simplified vocal tract model for excised larynx experiments," *Journal of Voice*, vol. 27, pp. 261–266, 5 2013.

[11] K. Migimatsu and I. T. Tokuda, "Experimental study on nonlinear source–filter interaction using synthetic vocal fold models," *The Journal of the Acoustical Society of America*, vol. 146, pp. 983–997, 8 2019.

[12] L. Oren, S. Khosla, and E. Gutmark, "Intraglottal geometry and velocity measurements in canine larynges," *The Journal of the Acoustical Society of America*, vol. 135, pp. 380–388, 1 2014.

[13] L. Oren, S. Khosla, and E. Gutmark, "Intraglottal pressure distribution computed from empirical velocity data in canine larynx," *Journal of Biomechanics*, vol. 47, pp. 1287–1293, 4 2014.

[14] A. Lodermeyer, S. Becker, M. Döllinger, and S. Kniesburges, "Phase-locked flow field analysis in a synthetic human larynx model," *Experiments in Fluids*, vol. 56, p. 77, 4 2015.

[15] A. Lodermeyer, M. Tautz, S. Becker, M. Döllinger, V. Birk, and S. Kniesburges, "Aeroacoustic analysis of the human phonation process based on a hybrid acoustic piv approach," *Experiments in Fluids*, vol. 59, p. 13, 1 2018.

[16] A. Lodermeyer, E. Bagheri, S. Kniesburges, C. Näger, J. Probst, M. Döllinger, and S. Becker, "The mechanisms of harmonic sound generation during phonation: A multi-modal measurement-based approach," *The Journal of the Acoustical Society of America*, vol. 150, pp. 3485–3499, 11 2021.

[17] C. F. de Luzan, L. Oren, A. Maddox, E. Gutmark, and S. M. Khosla, "Volume velocity in a canine larynx model using time-resolved tomographic particle image velocimetry," *Experiments in Fluids*, vol. 61, p. 63, 2 2020.

[18] R. C. Scherer, D. Shinwari, K. J. D. Witt, C. Zhang, B. R. Kucinschi, and A. A. Afjeh, "Intraglottal pressure profiles for a symmetric and oblique glottis with a divergence angle of 10 degrees," *The Journal of the Acoustical Society of America*, vol. 109, pp. 1616–1630, 4 2001.

[19] S. L. Thomson, L. Mongeau, and S. H. Frankel, "Aerodynamic transfer of energy to the vocal folds," *The Journal of the Acoustical Society of America*, vol. 118, pp. 1689–1700, 9 2005.

[20] M. Sondhi and J. Schroeter, "A hybrid time-frequency domain articulatory speech synthesizer," *IEEE Transactions on Acoustics, Speech, and Signal Processing*, vol. 35, pp. 955–967, 7 1987.

[21] B. H. Story, A.-M. Laukkanen, and I. R. Titze, "Acoustic impedance of an artificially lengthened and constricted vocal tract," *Journal of Voice*, vol. 14, pp. 455–469, 12 2000.

[22] J. L. Flanagan, *Speech Analysis, Synthesis and Perception*. Springer-Verlag, 1972.

[23] P. J. Schmid, "Dynamic mode decomposition of numerical and experimental data," *Journal of Fluid Mechanics*, vol. 656, pp. 5–28, 8 2010.

[24] C. Näger, A. Lodermeyer, and S. Becker, "Charakterisierung der Stimmlippenvibration an einem synthetischen Larynx-Modell mittels Laser-Scanning-Vibrometrie," *Fortschritte der Akustik - DAGA 2022*, pp. 927–930, 2022.